EANM 2023 – Vienna
ePoster: Cerianna / AIQ
Link: https://services.eanm.org/Modules/Presentation/Submission/overview.aspx

Must not exceed 4000 characters per section (excluding title and authors)

Add up to 7 media files with a maximum of 20.0 MB each. Acceptable formats: jpg, png, avi, mp4.

Title: **Automated Lesion Detection for ^{18}F-Fluoroestradiol PET/CT Images Demonstrates Lesion Heterogeneity in Patients with ER+ Metastatic Breast Cancer**

Authors: Kristen Wangerin, PhD[1]; Renee Miller, PhD[1], **Mark Battle, BSc[1]***; S Sean Houshmandi, PhD[2]; Daniel T Huff, PhD[2]; Amy J Weisman, PhD[2]; Timothy G Perk[2], PhD, Gary Ulaner, MD, PhD[3].

1 – GE HealthCare
2 – AIQ Solutions, Madison, WI, USA
3 — Hoag Family Cancer Institute
*Presenting Author

Aim/Introduction:

Breast cancer is the most common form of cancer in women.

- More than 70% of primary breast cancers express the estrogen receptor (ER)[1].

Interestingly, this expression of ERs in the primary lesion changes as the disease progresses. Additionally, discordance can be seen between primary and metastases in 18-55% of patients[2].

- Varying ER status between lesions within individual cancer patients is increasingly recognized as a cause of hormone therapy resistance in a metastatic setting[3].

^{18}F-fluoroestradiol ([^{18}F]FES, CERIANNA) is a positron emission tomography (PET) radiotracer which detects ER-positive lesions.

- [^{18}F]FES PET is indicated for use with PET imaging for the detection of ER-positive lesions as an adjunct to biopsy in patients with recurrent or metastatic breast cancer[4].
- [^{18}F]FES PET imaging offers a minimally invasive visual assessment of functional status of any tissue expressing ERs, including malignancies and their metastases.

[^{18}F]FES has clinical utility in the assessment of ER+ status in lesions that are difficult to biopsy[5].

- Due to the invasive nature of the procedure and location of some metastasis, sometimes only limited tissue samples are obtained, per patient.
- There are also difficulties in processing biopsy specimens, in particular for bone biopsy.
- Clinical decisions are based on the biopsy of the most accessible lesion, making decisions about the whole disease burden based on this only assessment that may not be representative of the ER status of all lesions (as illustrated in Fig. 1).

[^{18}F]FES is also appropriate for use when helping choose the most suitable therapy for patients according to their ER status.

- Determining ER status in lesions is key to a patient's clinical management.
- ER-positive tumours are more likely to respond to anti-hormonal therapeutics and have more favourable prognosis[6].

[^{18}F]FES is also of benefit when helping to resolve clinical dilemmas in cases where results are inconclusive by conventional assessment.

- Other imaging tests, including [^{18}F]FDG, diagnostic CT or bone scintigraphy, may provide equivocal or suspicious results.
- Therefore, a follow-up [^{18}F]FES exam may help to confirm equivocal lesions or highlight previously unseen lesions on standard imaging tests.

However, for each of these applications of [^{18}F]FES the manual detection, quantification and matching of lesions in patients with metastatic breast cancer is not feasible beyond a research setting. This is due in part to the duration and complexity of the process. As well as manually contouring all lesions, time taken to match lesions (needed to assess concordance) alone has been shown to take anywhere from 5 minutes (for low-burden cases) to around 60 minutes or more for a high-burden patient[7]. In contrast, an automated model has been reported to perform the same process in around 5 minutes.

This research presents a pilot study to evaluate a tool for automating lesion detection and assessing disease burden, through comparing [^{18}F]FES with other standard imaging modalities such as [^{18}F]FDG PET and CT, potentially increasing the clinical value of [^{18}F]FES PET imaging.

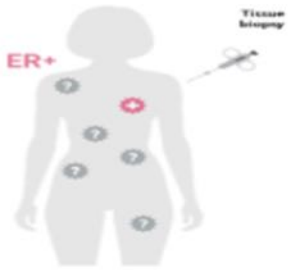

Fig. 1:
Illustration of tumour heterogeneity within a patient, demonstrating that a single biopsy may not be representative of the Estrogen Receptor status in disease as a whole

Note: Figures need to be added individually.
Tool allows annotation for each image
Statement of Source/Copyright information must be included before submission.
I used the following (From User Training Slides):
"© 2023 GE HealthCare. GE is a trademark of General Electric Company used under trademark license"

Materials and Methods:

An AI model, previously developed to detect lesions from 68Ga-DOTATATE PET/CT, was applied in this work to detect and segment [^{18}F]FES -positive lesions[8,9].

- [^{18}F]FES images, and corresponding CT or [^{18}F]FDG, for 52 patients with metastatic breast cancer were assessed by an expert radiologist and all lesions were manually contoured.
- Lesions were classified as one of two categories: “malignant”; abnormal characteristics identified on both [^{18}F]FES and CT/[^{18}F]FDG image, or “equivocal”; abnormal characteristics present on only one modality.
- These images were used as the ground truth for model training.

A convolutional neural network (Retina U-net) was then trained to automatically detect lesions on these images[10].

- Five-fold cross-validation was applied.

Model performance was assessed through lesion sensitivity and false positive rate compared to reader results.

- Lesion sensitivity was defined as the proportion of lesions present in the images as defined by the reader that were correctly identified by the algorithm.

An image registration and lesion matching step was used to measure concordance between lesions identified in two different image modalities.

- Inter-modality concordance of [^{18}F]FES (Cerianna) PET/CT to either CT or [^{18}F]FDG PET/CT was performed using TRAQinform technology (AIQ Solutions) (Fig. 2).
- Then, quantification of lesion overlap was used to label corresponding lesions in each modality.
- Analysis of the images for concordance was performed on a subset of cases: [^{18}F]FES with CT (n=13) and [^{18}F]FES with [^{18}F]FDG (n=13).
- Example concordance maps for two patients are shown for [^{18}F]FES & CT (Fig. 3) and [^{18}F]FES & FDG (Fig. 4).

Mediafiles for this section
Add up to 7 media files with a maximum of 20.0 MB each. You can upload .jpg, .png, .avi, .mp4.

Fig. 2

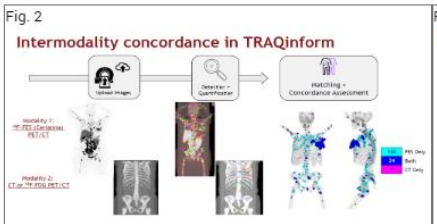

Automated model allows lesion detection and segmentation. Registration between different modalities offers ability to determine concordance in lesion detection.

AIQ Solutions, Madison, WI, USA.

EDIT REMOVE

Fig. 3

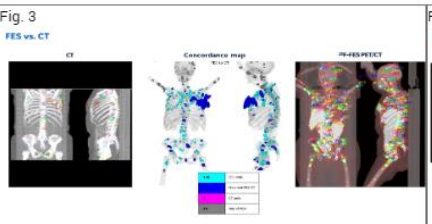

Example case of a concordance map between [18F]FES and CT

EDIT REMOVE

Fig. 4

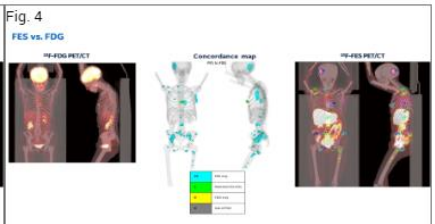

Example case of a concordance map between [18F]FES and [18F]FDG

EDIT REMOVE

+ ADD FILE

Results:

Lesions were detected in 51/52 patient [^{18}F]FES images that were subsequently used for training

- One patient had no [^{18}F]FES-avid lesions detected manually, but did have 2 [^{18}F]FDG lesions detected.
- On average, manual contouring took around 50 minutes per scan.

Overall model performance gave a median sensitivity of 62% compared to the reader, with a median false positive rate of 0 (Fig. 5).

- Perfect performance (100% lesion detection with no false positives) was achieved in 10/51 subjects.
- The median sensitivity and performance were improved when excluding "equivocal" lesions (Sensitivity: 100%, Performance: 18/33), lesions with a volume <0.5 cm^3 (Sensitivity: 100%, Performance: 15/28) or where contrast (SUV_{max}) was <2.5 (Sensitivity: 83%, Performance: 18/48).

Figures 6 and 7 demonstrate the utility of the tool to register and compare images from different modalities.

- After image registration and lesion matching, the number of lesions identified in each modality were counted.
- The number of lesions found by each imaging modality were plotted separately as well as the number of lesions found by both.
- As an example, in Case 1002 where images were available for all three modalities, 2 lesions were identified on CT, of which 1 was matched on [^{18}F]FES, and that lesion was also detected by [^{18}F]FDG.

Mediafiles for this section

Add up to 7 media files with a maximum of 20.0 MB each. You can upload .jpg, .png, .avi, .mp4.

Fig. 5

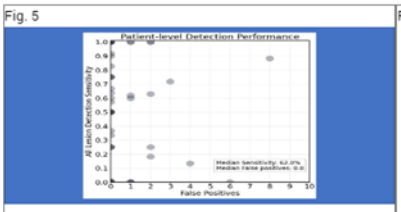

Plot showing sensitivity against positivity rate for 52 patients. The model performed well, with lesions detected in 51 out of 52 patients. The model performed with a perfect score (all lesions detected with no false positives) in 10 patients.

EDIT REMOVE

Fig. 6

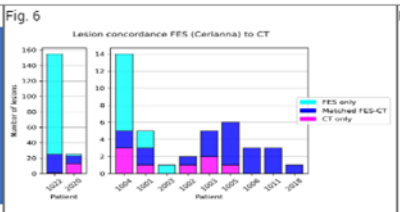

Concordance between the number of lesions detected by the model on both [18F]FES (CERIANNA) and CT images from the same patient. Two cases marked equivocal lesions in both modalities and are not shown.

EDIT REMOVE

Fig. 7

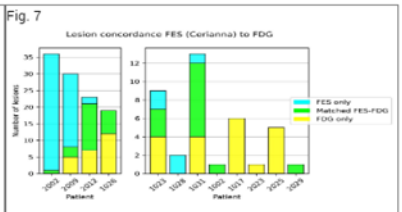

Concordance between the number of lesions detected by the model on both [18F]FES (CERIANNA) and [18F]FDG images from the same patient. One case marked equivocal lesions in both modalities and is not shown.

EDIT REMOVE

+ ADD FILE

Conclusion:

The AI model for identifying lesions in [^{18}F]FES images performed well, although trained on a limited data set. The accuracy improved for detection of larger volume, higher contrast and non-equivocal lesions. Further validation of the model with additional patient data is required for future use .

The model has the utility to support [^{18}F]FES readers to quickly identify all detected lesions for evaluation, with previous studies showing model performance for automated contouring and matching to be significantly more efficient than manual assessment. Although there is a substantial time difference (potentially ~2 hours down to 5 mins), automation is really the *only* option to make this type of assessment available as a clinical application.

Concordance was also demonstrated between modalities ([^{18}F]FES vs CT and [^{18}F]FES vs [^{18}F]FDG), utilising a deformable registration applied to the attenuation CT in order to register the two data sets. This allows the visualization of lesion characteristics between modalities in one tool.

Therefore, the combination of automated lesion detection combined with image registration could be useful for efficient evaluation of [^{18}F]FES images.

References:

1. Kurland BF, Wiggins JR, Coche A, *et al*. Whole-Body Characterization of Estrogen Receptor Status in Metastatic Breast Cancer with 16α-18F-Fluoro-17β-Estradiol Positron Emission Tomography: Meta-Analysis and Recommendations for Integration into Clinical Applications. Oncologist 2020;25:835–844.

2. van Kruchten M, Glaudemans A, de Vries E, *et al*. PET Imaging of Estrogen Receptors as a Diagnostic Tool for Breast Cancer Patients Presenting with a Clinical Dilemma. Journal of Nuclear Medicine, Vol. 53, No. 2, February 2012.

3. Dagogo-Jack I and Shaw AT. Tumour heterogeneity and resistance to cancer therapies. Nature Reviews: Clinical Oncology, Volume 15, February 2018, 81.

4. National Comprehensive Cancer Network (NCCN) Clinical Practice Guidelines in Oncology®. Breast Cancer. Version 4.2023 – March 23, 2023. https://www.nccn.org

5. Appropriate Use Criteria (AUC) for [^{18}F]FES PET. Society of Nuclear Medicine & Molecular Imaging (SNMMI). https://www.snmmi.org/auc

6. Ulaner GA. 16α-18F-fluoro-17β-Fluoroestradiol (FES): Clinical Applications for Patients With Breast Cancer. Seminars in Nuclear Medicine 2022;52(5):574-583.

7. Huff DT, Santoro-Fernandes V, Chen S, *et al*. Performance of an automated registration-based method for longitudinal lesion matching and comparison to inter-reader variability. Physics in Medicine and Biology. 2023 Aug 11.

8. Weisman A, Lokre O, Schott B, *et al*. Automated detection and quantification of neuroendocrine tumors on 68Ga-DOTATATE PET/CT images using a U-net ensemble method. Journal of Nuclear Medicine 63:3215–3215, 2022.

9. Weisman A, La Fontaine M, Lokre O, *et al*: Impact of Training with Data From Multiple Disease Types On Lesion Detection Performance in Two CNN Architectures. Medical Physics, pp E694–E694.

10. Jaeger PF, Kohl SA, Bickelhaupt S, *at al*. Retina U-Net: Embarrassingly simple exploitation of segmentation supervision for medical object detection. Machine Learning for Health Workshop, 2020, April. pp. 171-183. PMLR..